ACS EARTH AND SPACE CHEMISTRY

http://pubs.acs.org/journal/aesccq

Article

Volatility Change during Droplet Evaporation of Pyruvic Acid

Sarah S. Petters,* Thomas G. Hilditch, Sophie Tomaz, Rachael E. H. Miles, Jonathan P. Reid, and Barbara J. Turpin

Cite This: *ACS Earth Space Chem.* 2020, 4, 741−749

Read Online

ACCESS | Metrics & More | Article Recommendations | Supporting Information

ABSTRACT: Atmospheric water-soluble organic gases such as pyruvic acid are produced in large quantities by photochemical oxidation of biogenic and anthropogenic emissions and undergo water-mediated reactions in aerosols and hydrometeors. These reactions can contribute to aerosol mass by forming less-volatile compounds. Although progress is being made in understanding the relevant aqueous chemistry, little is known about the chemistry that takes place during droplet evaporation. Here, we examine the evaporation of aqueous pyruvic acid droplets using both the vibrating orifice aerosol generator (VOAG) and an electrodynamic balance (EDB). In some cases, pyruvic acid was first oxidized by OH radicals. The evaporation behavior of oxidized mixtures was consistent with expectations based on known volatilities of reaction products. However, independent VOAG and EDB evaporation experiments conducted without oxidation also resulted in stable residual particles; the estimated volume yield was 10−30% of the initial pyruvic acid. Yields varied with temperature and pyruvic acid concentration across cloud-, fog-, and aerosol-relevant concentrations. The formation of low-volatility products, likely cyclic dimers, suggests that pyruvic acid accretion reactions occurring during droplet evaporation could contribute to the gas-to-particle conversion of carbonyls in the atmosphere.

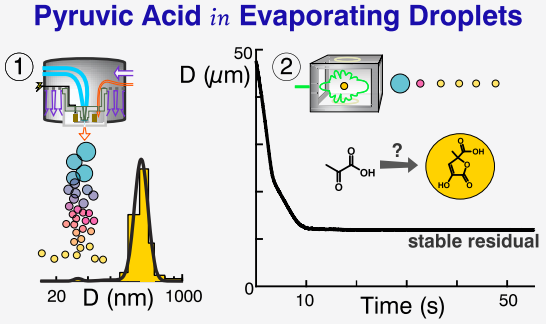

KEYWORDS: *secondary organic aerosol, multiphase chemistry, aerosol chemistry, aqSOA, carbonyl, vibrating orifice aerosol generator, aldol, cloud processing*

1. INTRODUCTION

Aerosols affect global climate and impact air quality, human health, and visibility. A substantial fraction of aerosol mass is organic, much of which is formed in situ in the atmosphere. Despite its ubiquity, predictions of secondary organic aerosol (SOA) formation rely on incomplete mechanisms unlikely to capture aerosol production over a wide range of precursors and conditions.[1−3] Water-mediated reactions, occurring in humidified aerosols, fogs, and cloud droplets, play an important role in converting water-soluble organic gases (WSOGs) to SOA mass.[4−6] However, the contribution of aqueous reactions to SOA mass remains uncertain in part because of a limited understanding of precursors and limited laboratory results to parameterize models.[1,7−11] Quantifying the impacts of aqueous and multiphase chemistry on aerosol mass remains challenging, and a more detailed understanding of product volatility is needed.

A significant fraction of low-molecular weight acids, aldehydes, and carbonyls dissolves into cloud or fog droplets. In the absence of additional reactions, these WSOGs largely evaporate during water evaporation; the trace amounts that remain in the aerosol phase are determined by their partial pressure in the gas phase and activity in the aerosol matrix. However, multiphase reactions can generate low-volatility products that are retained in the equilibrated aerosol. Several important criteria determine whether aqueous processing can appreciably increase SOA mass: (1) the precursor must be abundant, (2) it must have a high vapor pressure before aqueous reactions, (3) it must have a high Henry's law coefficient and thus strongly partition into water, and (4) it must react in the aqueous phase to form less-volatile products.

To date, many cloud- and fog-relevant studies have focused on the aqueous OH oxidation of a limited number of compounds meeting the above criteria, such as glyoxal,[12−14] glycolaldehyde,[15,16] methacrolein,[17] acetic acid,[18] methylglyoxal,[19−21] methyl vinyl ketone,[22] phenolic compounds,[23] and pyruvic acid,[24,25] and on oxidation by singlet molecular oxygen[23] and triplet excited states of oxygen,[23,26] photosensitization,[27] and photo-initiation.[28] The volatility of the products, or the extent to which products remain in the particle phase after water evaporation, has been determined for some of these systems but not for pyruvic acid. Studies have also shown that nonradical reactions can yield low-volatility compounds in deliquescent aerosols,[29−32] especially for

Received: February 11, 2020
Revised: April 1, 2020
Accepted: April 1, 2020
Published: April 1, 2020

glyoxal, methylglyoxal, and isoprene-derived epoxydiols.[29−32] Because these systems rely on catalysis, the formation of oligomers is sometimes reversible; irreversible formation of low-volatility products is generally associated with radical-[4,33,34] or ring-opening[31] reactions because of their higher activation energy. Nevertheless, glyoxal and methylglyoxal form stable products in evaporating solutions with or without inorganic catalysts[30,32,35] because of the reactive dicarbonyl group.[35] These and other accretion reactions occurring in the absence of photo-oxidation have been recognized as an important contributor to organic aerosol.[36] Evaporation of droplets concentrates solutes, shifts the solution pH, and can allow enhanced surface partitioning of surface-active compounds over short timescales, enhancing reaction rates.[32,37−41] The droplet air−liquid interface may also accelerate reactions by confining molecules to specific orientations, enhancing their reactivity or acidity,[42−46] and molecular partitioning to the air−liquid interface and self-organization in the surface layer can affect gas uptake and reaction rates.[47,48]

Pyruvic acid is abundant in aerosols, fogs, and clouds and is produced[19,24,25,49,50] photochemically in the atmosphere[50,51] mainly through gas-phase oxidation of aromatic hydrocarbons,[52−54] biomass burning,[55] and aqueous OH oxidation of methylglyoxal.[49,56] Pyruvic acid has an intermediate volatility[34] and partitions between the gas and aerosol phases.[51,53,57] Studies of aqueous pyruvic acid processing have focused on photolysis[26,56,58] and OH-radical-initiated photo-oxidation.[24,25,59] Evidence for dark pyruvic acid accretion reactions from environmental chamber studies shows that partitioning of pyruvic acid and other acids or carbonyls to SOAs exceeds expectations based on their high vapor pressures.[52,60] Here, we extend these studies to include dark processing of pyruvic acid in evaporating cloud droplets.

2. METHOD

Pyruvic acid evaporation experiments followed two methods and spanned concentration ranges from 10 μM to 2 M. Vibrating orifice aerosol generator (VOAG)[61] evaporation and residual analysis (VERA) was performed for a series of solutions between 10 μM and 20 mM, a concentration range that reflects cloud concentrations and concentrations as cloud droplets evaporate. Additional pyruvic acid evaporation experiments were performed using an electrodynamic balance (EDB) at 2 M. The EDB concentration is relevant to deliquescent aerosols rather than clouds; the choice of concentrations for EDB experiments was dictated by instrumental constraints. For comparison, VERA experiments were also performed for other organic acids (10 μM to 20 mM) and for aqueous pyruvic acid after OH radical oxidation (300 μM pyruvic acid; fog-relevant concentration). An evaporation model was used to aid in the interpretation of the data. VERA and EDB techniques, oxidation experiments, and modeling are described in the following paragraphs.

2.1. VOAG Evaporation and Residual Analysis. Droplet evaporation experiments were performed for aqueous solutions of pyruvic acid (with and without OH oxidation) or other organic acids/carbonyls using VERA as described previously.[16] VERA emulates cloud droplet evaporation by generating micron-scale droplets with very narrow size distributions (monodispersed and near-cloud-relevant sizes)[62] and evaporating them in a turbulent flow tube. Briefly, a VOAG (TSI 3450) was used to generate monodisperse droplets. Water evaporated rapidly (~1 s) and size distributions of the organic residuals were detected in real time downstream with an aerosol spectrometer (GRIMM Aerosol Technik Ainring GmbH; model 1.109). Evaporation of the organic was used to quantify its vapor pressure. Modifications to the instrument liquid feed, orifice, and flow tube following Barr et al.[63−65] are described in the Supporting Information alongside the measurement schematic (Figure S1); analysis is described below. A 20 μm orifice was used and produced 35 ± 0.053 μm droplets under typical conditions. For an involatile solute, solutions of 9.4 μM to 19 mM result in dry residual diameters (hereafter referred to as "nominal diameters") of 0.30−3.9 μm. Equilibrium water retention was estimated from the molar volume[66,67] and did not exceed 2−5% of the nominal particle volume. Calculation details and spectrometer calibration are described in the Supporting Information. Observed residual diameters were taken as the peak of the measured size distribution. The evaporation process and the influence of physicochemical properties are described in the Evaporation Model section below.

2.2. Evaporation in the EDB. Pyruvic acid solutions were evaporated in an EDB as described previously.[68−70] Aqueous solutions of 2 M pyruvic acid in ultrapure water were prepared. The higher concentration was necessary because of experimental constraints and is comparable to total organic carbon (TOC) in deliquescent aerosols.[71] Droplets were produced using a piezoelectric droplet-on-demand generator and trapped in an electrodynamic potential well generated from two pairs of concentric cylindrical electrodes. Trapped droplets evaporated in a 3 cm s^{-1} N_2 gas flow at constant temperature and relative humidity (RH). A green laser (532 nm) illuminated the droplet and the scattered diffraction pattern was used to determine the droplet size with a time resolution of 10 ms. Experiments were performed at 10, 20, and 25 °C. Additional tests included variable RH or a different initial solvent. EDB experiments were conducted at the University of Bristol. Each experiment was repeated 4−9 times.

2.3. Oxidation and Product Quantification for Pyruvic Acid + OH(aq). Aqueous solutions of 300 μM (10.8 ppm-C) pyruvic acid were oxidized via OH radicals using a water-jacketed 1 L photochemical batch reactor at 25 °C as described previously and products were quantified by ion chromatography.[19,72] The pyruvic acid concentration is similar to the TOC found in fog water or polluted cloud water.[73,74] Estimated steady-state [OH] was ~5.5×10^{-12} M during pyruvic acid oxidation.[75] Additional experimental details are provided in the Supporting Information. Typical cloud water [OH] is believed to be 10^{-13} M or lower.[76,77] We used higher concentrations to focus on OH-initiated reactions and to access a wide range of equivalent atmospheric oxidation timescales from minutes to days.[76]

Aliquots of 10−12 mL were withdrawn at increasing time intervals, and offline analysis was performed within one day. Samples were analyzed for organic acids using ion chromatography (IC; Dionex ICS-3000) and for TOC (Sievers M9). Evaporation experiments using VERA were performed for a subset of aliquots directly and after serial dilution.

2.4. Evaporation Model. Evaporation of pyruvic acid solution droplets in VERA was estimated following Su et al.[70,78] and Bilde et al.[79,80] A model description is included in the Supporting Information. Particle velocity relative to the gas was assumed to be the terminal settling velocity[80] and the gas-phase concentration of the organic was assumed to be zero in the flow tube (we estimate it was <2% saturated). Pyruvic acid

https://dx.doi.org/10.1021/acsearthspacechem.0c00044
ACS Earth Space Chem. 2020, 4, 741−749

diffusivity in air was estimated to be 8.1×10^{-2} cm^2 s^{-1} via the Hirschfelder equation.[79,81,82] VERA was emulated by modeling water evaporation from the droplet until reaching the organic nominal residual diameter, followed by modeling organic evaporation until the time of observation with the spectrometer. Modeled RH was 11% and measured RH was 10−13%. In addition to modeling binary water−organic solutions, we modeled scenarios introducing a second solute with lower vapor pressure (10^{-4} Pa) into the droplet. The modeled residual diameter is mainly controlled by aqueous solution concentration, organic vapor pressure, evaporation time and RH.

Figure S2 shows the evaporation model for the VERA technique. After water evaporation, the "nominal diameter" of the residual organic particle is calculated from the initial solution concentration assuming no evaporation of the organic (x-axis). However, because the organic matter partially evaporates, the "observed diameter" (residual diameter observed with the spectrometer), on the y-axis, is dependent on the organic vapor pressure.

Panel A shows the expected "observed diameter" for a pyruvic acid-like compound with different assigned vapor pressures. The lines bend because evaporation is proportional to the droplet surface area. The line spacing shows the vapor pressure resolution for organics of similar size and functionality. Vapor pressures (p^o) between 3 and 0.3 Pa are resolved under current operating conditions. Panel B shows the result of adding an involatile second solute to the modeled droplets, simulating the conversion of some of the pyruvic acid to a less volatile compound—one that does not evaporate on the timescale of the measurement. The inset is a three-bin volatility basis set for this setup, where bin 1 ($p^o \leq 0.3$ Pa) describes compounds that do not evaporate, bin 2 ($0.3 \leq p^o \leq 3$ Pa) describes compounds that partially evaporate, and bin 3 ($p^o \geq 3$ Pa) describes compounds evaporating completely before detection.

Figure S2 shows the droplet size after 4.9 s of evaporation (the flow tube residence time), to simulate what is measured by VERA. It does not show the time-resolved evaporation of multiple solution components because VERA uses a fixed observation time and multiple experiments with different concentrations to generate a plot of the nominal versus observed diameter. The model is therefore helpful in interpreting the data. The presence or absence of curvature in the observations is an indication of the volume fraction of the solute in each of the volatility bins shown in panel B. If observations include curvature, some component falls in bin 2 and its vapor pressure can be determined with greater precision. In the absence of curvature, all components are in bins 1 and 3, with the fraction in bin 1 shown by the angle of the line of observed diameters. For example, if the angle is 0° (x-axis), all compounds are in bin 3 (evaporated), and if the angle is 45° (1:1 line), all compounds are in bin 1 (did not evaporate). Evaporation data (nominal vs observed residual diameter) falling on a line between 0 and 45° in Figure S2 panel B are fitted, and the slope of the fit line is indicative of the fraction of organic that did not evaporate.

3. RESULTS AND DISCUSSION

In the following paragraph, we show that OH oxidation of pyruvic acid slowly produces acetic and oxalic acids, consistent with known mechanisms and that oxidation reduces the volatility of the mixture. Then, we present the dark evaporation of aqueous pyruvic acid using VERA and EDB techniques. Despite expectations based on the vapor pressure of pyruvic acid, droplet evaporation resulted in the formation of stable residual particles. A possible oligomerization mechanism and atmospheric implications are discussed.

3.1. Oxidation Experiments. Figure 1 shows the evolving composition of 300 μM aqueous pyruvic acid undergoing OH

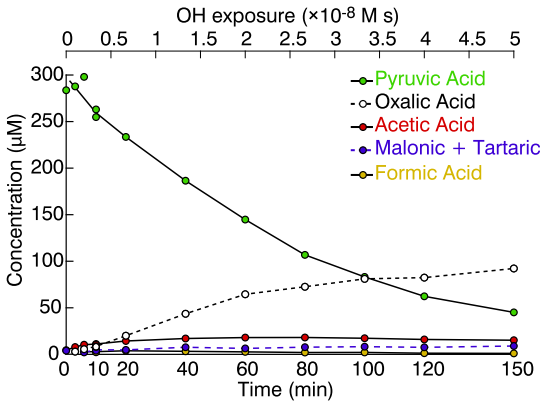

Figure 1. Oxidation products of pyruvic acid + OH(aq) as quantified by ion chromatography.

radical-initiated oxidation over 150 min, as determined by ion chromatography. Oxidation converts pyruvic acid mainly to oxalic and acetic acid. This delayed formation of oxalic acid is consistent with the known multistep oxidation mechanisms.[19,75,83] Evaporation of these solutions and their volatility is discussed below.

3.2. VERA Evaporation Experiments. Figure 2 shows the results of VERA experiments for oxidized pyruvic acid and for (dark) standard solutions of pyruvic acid or other organics. As oxidation converts pyruvic acid to oxalic acid, the net result is lower volatility, as seen by an increase in the slope in Figure 2A. By comparing the slope of the observations with the modeled lines, we estimate that the volume fraction of organics in volatility bin 1 ($p^o < 0.3$ Pa) was ~60% after 150 min of oxidation. The remaining 40% was likely unreacted pyruvic acid and volatile products such as acetic and formic acids. Panel B shows evaporated standard solutions. Most organics longer than three carbons did not evaporate before observation and thus fall in bin 1 and are observed on the 1:1 line. Additional experiments falling on the 1:1 line were omitted for clarity (glyoxal, glyoxylic acid, and malic acids). Compounds evaporating completely fall in bin 3 ($p^o > 3$) and are observed on the x-axis. Pyruvic acid solutions evaporated partially (dark blue). As described in Section 3, the lack of curvature in the observation indicates that some of the solute was volatile (pyruvic acid falls in volatility bin 3) and some of the solute did not evaporate (unknown compound falling in volatility bin 1). Assuming volume additivity, ~10 ± 5% of the pyruvic acid by volume was converted to a lower volatility product. The volume conversion is likely lower when accounting for solvation effects.

Figure 2C shows that oxidation shifted products into the lower-volatility bin (bin 1). Colored circles indicate the fitted slope of VERA experiments in panel A and the black line is an independent estimate of nonevaporating compounds for the same mixtures using ion chromatography, as shown in Figure 1. The close agreement between these two estimates of evaporation corroborates the VERA model. The exception is

https://dx.doi.org/10.1021/acsearthspacechem.0c00044
ACS Earth Space Chem. 2020, 4, 741−749

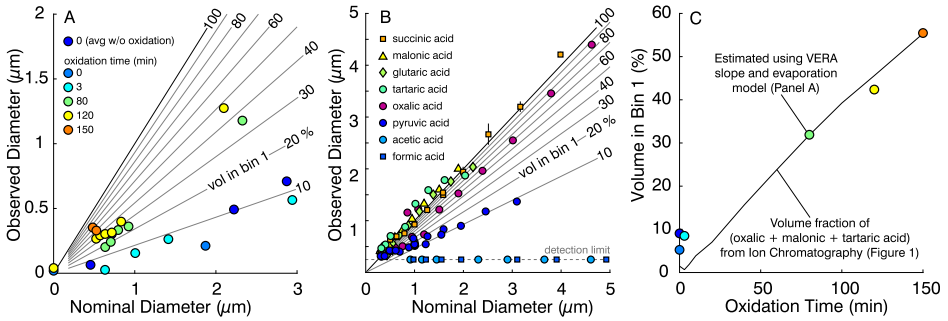

Figure 2. VERA evaporation of (A) oxidized pyruvic acid solutions (background subtracted) and (B) aqueous pyruvic acid and other compounds. The observed diameter is with a spectrometer and nominal diameters are involatile-equivalent diameters from solution concentration. Grey lines show estimated fraction with lower volatility (volatility bin 1; $p^o < 0.3$ Pa). (C) Percentage of the solute in bin 1 ($p^o < 0.3$) estimated independently from the VERA slope (circles; data from panel A) and from IC data (line; data from Figure 1).

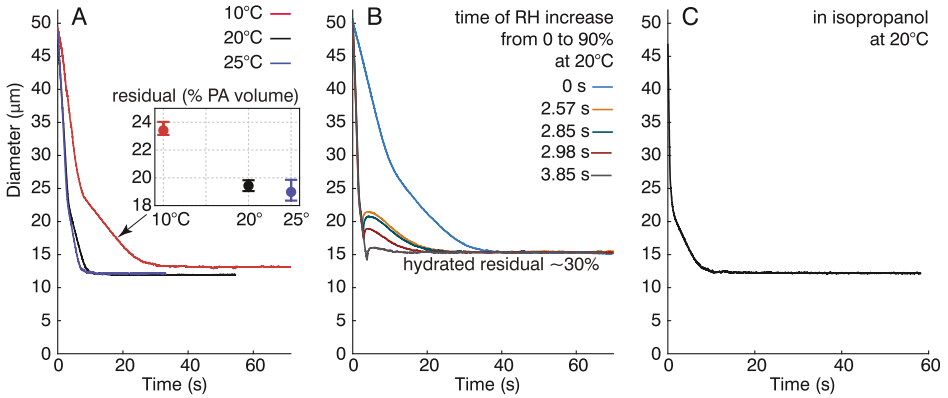

Figure 3. Evaporation of 0.1 mass fraction pyruvic acid solution droplets as observed with the EDB. (A) Aqueous pyruvic acid evaporating in dry N_2 at three gas-phase temperatures (inset) residual volumes at different temperatures. (B) Aqueous pyruvic acid response to abruptly increasing RH during evaporation (at different times as indicated), (C) pyruvic acid in isopropanol evaporating at 20 °C.

near 0 min of oxidation, where evaporation of the pyruvic acid produced a 10% unknown residual (see blue circles, Figure 2C). Further experiments investigating this phenomenon were performed using the EDB and are detailed below.

3.3. EDB Evaporation Experiments. Figure 3 shows the evaporation of pyruvic acid solutions in the EDB. The sequential evaporation of water and pyruvic acid followed by the retention of an unknown low-volatility substance is clearly delineated by two sharp changes in the evaporation rate (panel A). The evaporation rate slowed as remaining droplet constituents became less volatile. Abruptly raising the RH did not change the final residual diameter (panel B). In the evaporation of pyruvic acid + isopropanol (panel C), the sequential evaporation of the solvent and pyruvic acid is also observed, again resulting in a less-volatile residual. The volume conversion of pyruvic acid to a low-volatility residual (assuming volume additivity and constant density equal to that of pyruvic acid) was ~15−30% across all EDB experiments.

Varying experimental conditions affected the production of the low-volatility component. Figure 3A shows that the residual volume of the low-volatility product increases at colder temperatures, demonstrating that the sustained period of high pyruvic acid concentration in the evaporating droplet has a greater effect on the reaction rate than the reduction in molecular collisions expected at low temperatures. The volatility of the residual remained below the limit of quantification by EDB ($<5 \times 10^{-3}$ Pa) at all temperatures. Additional experiments operating on much longer timescales would have been necessary to quantify the evaporation of the formed particles. Although vapor pressure increases with increasing temperature, the effect of temperature-dependent vapor pressure on the evaporation of a single compound would result in different evaporation rates and not different yields. Higher initial droplet concentrations using the same initial droplet size (VERA vs EDB) doubled the volumetric yield. When RH was increased from 0 to 90% at different times during droplet evaporation (Figure 3B), the observed residual diameter was unchanged. Note that the residual here is larger because of equilibrium water uptake (hygroscopicity estimate of $\kappa \approx 0.015$,[84] which is comparable to that of larger molecules found in SOA[85]). This indicates that changing the hygroscopically bound water in the evaporating pyruvic acid solution does not speed up the low-volatility product formation. In panel C, evaporating the pyruvic acid in pure isopropanol resulted in evaporation rates and residuals similar to those of aqueous solutions but a little higher (23 ± 1% residual), perhaps reflecting slightly different chemistry. Because carbonyls do not undergo hydration reactions to form gem-diols as readily in isopropanol as they do in water, this suggests that the reaction producing the residual is not accelerated by the formation of a gem-diol as observed for glyoxal.[35]

3.4. Proposed Mechanism for Self-Reaction of Pyruvic Acid. Potential formation mechanisms and structures of a low-volatility residual are now discussed. The residual volume is larger than the stated pyruvic acid impurity of 2% (all EDB experiments used brand-new stock), and several independent sources of pyruvic acid standards produced

https://dx.doi.org/10.1021/acsearthspacechem.0c00044
ACS Earth Space Chem. 2020, 4, 741−749

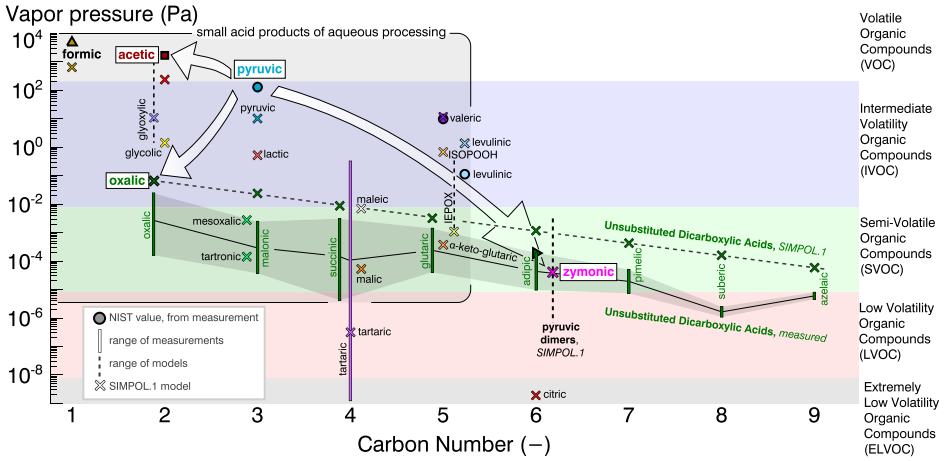

Figure 4. Vapor pressures of pyruvic acid reaction products compared to past organic measurements (20 °C),[110] SIMPOL.1[108] -estimated vapor pressures, and volatility ranges defined by Donahue et al.[34] Pyruvic dimers include several multifunctional cyclic acids (Figure S5).

similar results. Some of this residual may form in the stock solution prior to use; however, the changing volumetric yields with changing temperatures suggest that reactions occur during evaporation experiments. Evaporation rates of the low-volatility residual were below the detection limit; thus, the influence of temperature on vapor pressure did not affect the observed yield. Gas-phase impurities are ruled out with the EDB and are unlikely with VERA.

Pyruvic acid exists as several species in solution and these equilibria are shifted by the changing pH during evaporation. The carboxylic acid group can deprotonate to form the pyruvate anion and the keto group can hydrate to form a gem-diol or tautomerize to form an enol. At room temperature, roughly 10% of pyruvate or 60% of pyruvic acid forms a diol.[86] Equilibrium between these forms of pyruvic acid is complicated by the high surface-to-volume ratio and rapid removal of both water and the volatile carboxylic acid form of pyruvic acid during evaporation of droplets.[37,42,44]

The formation of C−O−C bonds by attack of an ROH group on the double bond of either the carboxyl group or the keto group of pyruvic acid is plausible,[36,87,88] and oligoester products in SOA have been observed in both laboratory and field studies.[89,90] For example, the gem-diol of a hydrated pyruvic acid molecule can attack the double bond of the carboxyl group of another pyruvic acid molecule. In isopropanol, the isopropanol can attack the carboxyl double bond, producing a similar ester (Figure 3C). Either isopropanol or the pyruvic gem-diol may attack the hydrated keto group of another pyruvic acid molecule, forming a hemiacetal and potentially repeating to form an acetal, as has been reported for glyoxal[91] and 2-methylglyceric acid.[89,90] Formation of an acetal may be promoted by the removal of pyruvic acid and water from the droplet during evaporation[92,93] and enhanced acidity and reactivity in the surface phase.[42,44,45]

Aldol addition and condensation reactions occur by the attack of the enol tautomer of pyruvic acid on a protonated keto group of another molecule. Aldol addition has been proposed as a thermodynamically favorable reaction in bulk aqueous systems[94−96] and these reactions are likely accelerated at the droplet surface[42,44,45] and by evaporation of water and pyruvic acid.[92,93] Figure S5 shows a proposed mechanism with a cyclic dimer as a potential end product of the aqueous evaporation experiments in this work. Pyruvic acid tautomerizes readily in solution,[97] and aldol addition can proceed without hydration of the keto group to a gem-diol. Self-reactions by aldol addition have been reported for evaporating aqueous droplets of methylglyoxal and glyoxal[30] and for pyruvic acid in both dark and photochemical reaction systems.[56,98]

3.5. Atmospheric Implications. Pyruvic acid has diverse removal processes in the atmosphere, where it can partition between aerosol, aqueous, and gas phases and can dissociate, hydrate, or tautomerize in solution. The primary source of pyruvic acid outside urban areas is the aqueous-phase OH oxidation of isoprene oxidation products such as methylglyoxal and lactic acid,[19,57,99] and under dry conditions, it is found largely in the gas phase (rather than the aerosol), where it is removed by direct photolysis and dry deposition.[51,53,100] In the presence of fogs and clouds, pyruvic acid can be retained by (or repartition back into) the aqueous phase because of its high water solubility (Henry's law constant of 3.1×10^5 M atm^{-1}).[101] The aqueous phase photochemistry is then competitive with the gas-phase direct photolysis as a sink for pyruvic acid.[102] In clouds and fogs, some pyruvic acid undergoes OH oxidation to yield acetic acid, CO_2, and oxalic acid through a glyoxylic acid intermediate.[19] Because of the multistep chemistry, conversion of pyruvic to oxalic acid takes hours and occurs over multiple cloud cycles or in a persistent fog. Aqueous dehydrated pyruvic acid is light-absorbing and can undergo direct photolysis or photosensitized reactions resulting in acetoin, lactic and acetic acid, and oligomers through the excited triplet state of the carbonyl oxygen.[26,28] However, dark reactions in clouds and fogs can also occur. Dicarbonyls similar to pyruvic acid such as glyoxal and methylglyoxal can oligomerize in evaporating droplets.[29,30,32,35,88] This work shows the potential for pyruvic acid to oligomerize during cloud and fog droplet evaporation.

Figure 4 depicts the volatility evolution of aqueous solutions of pyruvic acid. The box in the upper left-hand corner shows volatile and semivolatile carboxylic acids that are highly water soluble, often result from aqueous oxidation, and partition readily into droplets. Processes reducing the volatility of these compounds can increase the fraction of organic mass that remains in the particle phase after water evaporation. Among these is pyruvic acid, with a vapor pressure of ~10^2 Pa at 20 °C.[103,104] Aqueous OH-radical initiated oxidation, dark acid-catalyzed accretion reactions, and salt formation of pyruvic acid

https://dx.doi.org/10.1021/acsearthspacechem.0c00044
ACS Earth Space Chem. 2020, 4, 741−749

(not shown) have the potential to reduce the volatility of pyruvic acid. Aqueous OH oxidation of pyruvic acid forms acetic acid, glyoxylic acid, and subsequently oxalic acid, whose vapor pressure is in the semivolatile range (p^o = 10^{-2} to 10^{-4} Pa).[105,106] The preference of oxalic acid for the particle phase in the atmosphere is likely due to the formation of low-volatility oxalate salts or complexes.[4,12,107] This work suggests that evaporating pyruvic acid solution droplets at aerosol-, fog-, and cloud-relevant concentrations and atmospheric temperatures (10−25 °C) in the absence of an inorganic catalyst leads to the formation of acetals and/or cyclic dimers with estimated vapor pressures of 4 × 10^{-5} Pa[108] and 10−30% volumetric yields. This mechanism could compete with photochemical sinks for pyruvic acid during cloud cycling.

Although the vapor pressure of dimers of pyruvic acid is significantly lower than that of pyruvic acid, they are still considered semivolatile or low-volatility compounds. Dimerization enhances the partitioning of monomers to the condensed phase.[36] The formed dimers, especially those with unsaturated double bonds, can participate in additional condensed-phase reactions. For example, the pyruvic acid dimers shown in Figure S5 have been shown to partition to the air−water interface,[109] where they may have enhanced reactivity for subsequent reactions.[38] The formation of surface active unsaturated dimers from carbonyls such as pyruvic acid during cloud or fog evaporation is one way in which carbon can be transformed in the atmosphere and influence atmospheric chemistry.

■ ASSOCIATED CONTENT

Supporting Information

The Supporting Information is available free of charge at https://pubs.acs.org/doi/10.1021/acsearthspacechem.0c00044.

Instrument modifications and schematic; oxidation details; modeling details; and reaction mechanisms (PDF)

■ AUTHOR INFORMATION

Corresponding Author

Sarah S. Petters − *Department of Environmental Sciences and Engineering, Gillings School of Global Public Health, University of North Carolina at Chapel Hill, Chapel Hill NC 27599-7431, North Carolina, United States;* orcid.org/0000-0002-4501-7127; Email: spetters@unc.edu

Authors

Thomas G. Hilditch − *School of Chemistry, University of Bristol, Bristol BS8 1TS, U.K.*

Sophie Tomaz − *Department of Environmental Sciences and Engineering, Gillings School of Global Public Health, University of North Carolina at Chapel Hill, Chapel Hill NC 27599-7431, North Carolina, United States*

Rachael E. H. Miles − *School of Chemistry, University of Bristol, Bristol BS8 1TS, U.K.*

Jonathan P. Reid − *School of Chemistry, University of Bristol, Bristol BS8 1TS, U.K.;* orcid.org/0000-0001-6022-1778

Barbara J. Turpin − *Department of Environmental Sciences and Engineering, Gillings School of Global Public Health, University of North Carolina at Chapel Hill, Chapel Hill NC 27599-7431, North Carolina, United States*

Complete contact information is available at: https://pubs.acs.org/10.1021/acsearthspacechem.0c00044

Funding

This project was funded by the U.S. National Science Foundation Postdoctoral Fellowship under Award #AGS-1624696. R.E.H.M. was supported by the U.K. Engineering and Physical Sciences Research Council, grant number EP/N025245/1. S.T. and B.J.T. were supported by the U. S. National Oceanic and Atmospheric Administration under Award #NA16OAR4310106. We thank Sara Duncan for assistance with some of the experiments.

Notes

The authors declare no competing financial interest.

■ REFERENCES

(1) Mao, J.; Carlton, A.; Cohen, R. C.; Brune, W. H.; Brown, S. S.; Wolfe, G. M.; Jimenez, J. L.; Pye, H. O. T.; Lee Ng, N.; Xu, L.; McNeill, V. F.; Tsigaridis, K.; McDonald, B. C.; Warneke, C.; Guenther, A.; Alvarado, M. J.; de Gouw, J.; Mickley, L. J.; Leibensperger, E. M.; Mathur, R.; Nolte, C. G.; Portmann, R. W.; Unger, N.; Tosca, M.; Horowitz, L. W. Southeast Atmosphere Studies: Learning from Model-Observation Syntheses. *Atmos. Chem. Phys.* **2018**, *18*, 2615−2651.

(2) Chan Miller, C.; Jacob, D. J.; Marais, E. A.; Yu, K.; Travis, K. R.; Kim, P. S.; Fisher, J. A.; Zhu, L.; Wolfe, G. M.; Hanisco, T. F.; Keutsch, F. N.; Kaiser, J.; Min, K.-E.; Brown, S. S.; Washenfelder, R. A.; González Abad, G.; Chance, K. Glyoxal Yield from Isoprene Oxidation and Relation to Formaldehyde: Chemical Mechanism, Constraints from SENEX Aircraft Observations, and Interpretation of OMI Satellite Data. *Atmos. Chem. Phys.* **2017**, *17*, 8725−8738.

(3) Marais, E. A.; Jacob, D. J.; Jimenez, J. L.; Campuzano-Jost, P.; Day, D. A.; Hu, W.; Krechmer, J.; Zhu, L.; Kim, P. S.; Miller, C. C.; Fisher, J. A.; Travis, K.; Yu, K.; Hanisco, T. F.; Wolfe, G. M.; Arkinson, H. L.; Pye, H. O. T.; Froyd, K. D.; Liao, J.; McNeill, V. F. Aqueous-Phase Mechanism for Secondary Organic Aerosol Formation from Isoprene: Application to the Southeast United States and Co-Benefit of SO_2 Emission Controls. *Atmos. Chem. Phys.* **2016**, *16*, 1603−1618.

(4) Ervens, B.; Turpin, B. J.; Weber, R. J. Secondary Organic Aerosol Formation in Cloud Droplets and Aqueous Particles (AqSOA): A Review of Laboratory, Field and Model Studies. *Atmos. Chem. Phys.* **2011**, *11*, 11069−11102.

(5) Blando, J. D.; Turpin, B. J. Secondary Organic Aerosol Formation in Cloud and Fog Droplets: A Literature Evaluation of Plausibility. *Atmos. Environ.* **2000**, *34*, 1623−1632.

(6) Budisulistiorini, S. H.; Canagaratna, M. R.; Croteau, P. L.; Marth, W. J.; Baumann, K.; Edgerton, E. S.; Shaw, S. L.; Knipping, E. M.; Worsnop, D. R.; Jayne, J. T.; Gold, A.; Surratt, J. D. Real-Time Continuous Characterization of Secondary Organic Aerosol Derived from Isoprene Epoxydiols in Downtown Atlanta, Georgia, Using the Aerodyne Aerosol Chemical Speciation Monitor. *Environ. Sci. Technol.* **2013**, *47*, 5686−5694.

(7) McVay, R.; Ervens, B. A Microphysical Parameterization of AqSOA and Sulfate Formation in Clouds. *Geophys. Res. Lett.* **2017**, *44*, 7500−7509.

(8) Woo, J. L.; McNeill, V. F. SimpleGAMMA v1.0 − a Reduced Model of Secondary Organic Aerosol Formation in the Aqueous Aerosol Phase (AaSOA). *Geosci. Model Dev.* **2015**, *8*, 1821−1829.

(9) Heald, C. L.; Coe, H.; Jimenez, J. L.; Weber, R. J.; Bahreini, R.; Middlebrook, A. M.; Russell, L. M.; Jolleys, M.; Fu, T.-M.; Allan, J. D.; Bower, K. N.; Capes, G.; Crosier, J.; Morgan, W. T.; Robinson, N. H.; Williams, P. I.; Cubison, M. J.; DeCarlo, P. F.; Dunlea, E. J. Exploring the Vertical Profile of Atmospheric Organic Aerosol: Comparing 17 Aircraft Field Campaigns with a Global Model. *Atmos. Chem. Phys.* **2011**, *11*, 12673−12696.

(10) Carlton, A. G.; Turpin, B. J.; Altieri, K. E.; Seitzinger, S. P.; Mathur, R.; Roselle, S. J.; Weber, R. J. CMAQ Model Performance

Enhanced When In-Cloud Secondary Organic Aerosol Is Included: Comparisons of Organic Carbon Predictions with Measurements. *Environ. Sci. Technol.* **2008**, *42*, 8798−8802.
(11) Fu, T.-M.; Jacob, D. J.; Wittrock, F.; Burrows, J. P.; Vrekoussis, M.; Henze, D. K. Global Budgets of Atmospheric Glyoxal and Methylglyoxal, and Implications for Formation of Secondary Organic Aerosols. *J. Geophys. Res.: Atmos.* **2008**, *113*, D15303.
(12) Ortiz-Montalvo, D. L.; Häkkinen, S. A. K.; Schwier, A. N.; Lim, Y. B.; McNeill, V. F.; Turpin, B. J. Ammonium Addition (and Aerosol PH) Has a Dramatic Impact on the Volatility and Yield of Glyoxal Secondary Organic Aerosol. *Environ. Sci. Technol.* **2014**, *48*, 255−262.
(13) Carlton, A. G.; Turpin, B. J.; Altieri, K. E.; Seitzinger, S.; Reff, A.; Lim, H.-J.; Ervens, B. Atmospheric Oxalic Acid and SOA Production from Glyoxal: Results of Aqueous Photooxidation Experiments. *Atmos. Environ.* **2007**, *41*, 7588−7602.
(14) Tan, Y.; Perri, M. J.; Seitzinger, S. P.; Turpin, B. J. Effects of Precursor Concentration and Acidic Sulfate in Aqueous Glyoxal−OH Radical Oxidation and Implications for Secondary Organic Aerosol. *Environ. Sci. Technol.* **2009**, *43*, 8105−8112.
(15) Perri, M. J.; Seitzinger, S.; Turpin, B. J. Secondary Organic Aerosol Production from Aqueous Photooxidation of Glycolaldehyde: Laboratory Experiments. *Atmos. Environ.* **2009**, *43*, 1487−1497.
(16) Ortiz-Montalvo, D. L.; Lim, Y. B.; Perri, M. J.; Seitzinger, S. P.; Turpin, B. J. Volatility and Yield of Glycolaldehyde SOA Formed through Aqueous Photochemistry and Droplet Evaporation. *Aerosol Sci. Technol.* **2012**, *46*, 1002−1014.
(17) Michaud, V.; El Haddad, I.; Sellegri, K.; Laj, P.; Villani, P.; Picard, D.; Marchand, N.; Monod, A.; Liu, Y. In-Cloud Processes of Methacrolein under Simulated Conditions − Part 3: Hygroscopic and Volatility Properties of the Formed Secondary Organic Aerosol. *Atmos. Chem. Phys.* **2009**, *9*, 5119−5130.
(18) Tan, Y.; Lim, Y. B.; Altieri, K. E.; Seitzinger, S. P.; Turpin, B. J. Mechanisms Leading to Oligomers and SOA through Aqueous Photooxidation: Insights from OH Radical Oxidation of Acetic Acid and Methylglyoxal. *Atmos. Chem. Phys.* **2012**, *12*, 801−813.
(19) Tan, Y.; Carlton, A. G.; Seitzinger, S. P.; Turpin, B. J. SOA from Methylglyoxal in Clouds and Wet Aerosols: Measurement and Prediction of Key Products. *Atmos. Environ.* **2010**, *44*, 5218−5226.
(20) Lim, Y. B.; Turpin, B. J. Laboratory Evidence of Organic Peroxide and Peroxyhemiacetal Formation in the Aqueous Phase and Implications for Aqueous OH. *Atmos. Chem. Phys.* **2015**, *15*, 12867−12877.
(21) Ortiz-Montalvo, D. L.; Schwier, A. N.; Lim, Y. B.; McNeill, V. F.; Turpin, B. J. Volatility of Methylglyoxal Cloud SOA Formed through OH Radical Oxidation and Droplet Evaporation. *Atmos. Environ.* **2016**, *130*, 145−152.
(22) Renard, P.; Reed Harris, A. E.; Rapf, R. J.; Ravier, S.; Demelas, C.; Coulomb, B.; Quivet, E.; Vaida, V.; Monod, A. Aqueous Phase Oligomerization of Methyl Vinyl Ketone by Atmospheric Radical Reactions. *J. Phys. Chem. C* **2014**, *118*, 29421−29430.
(23) Yu, L.; Smith, J.; Laskin, A.; George, K. M.; Anastasio, C.; Laskin, J.; Dillner, A. M.; Zhang, Q. Molecular Transformations of Phenolic SOA during Photochemical Aging in the Aqueous Phase: Competition among Oligomerization, Functionalization, and Fragmentation. *Atmos. Chem. Phys.* **2016**, *16*, 4511−4527.
(24) Altieri, K. E.; Carlton, A. G.; Lim, H.-J.; Turpin, B. J.; Seitzinger, S. P. Evidence for Oligomer Formation in Clouds: Reactions of Isoprene Oxidation Products. *Environ. Sci. Technol.* **2006**, *40*, 4956−4960.
(25) Carlton, A. G.; Turpin, B. J.; Lim, H.-J.; Altieri, K. E.; Seitzinger, S. Link between Isoprene and Secondary Organic Aerosol (SOA): Pyruvic Acid Oxidation Yields Low Volatility Organic Acids in Clouds. *Geophys. Res. Lett.* **2006**, *33*, L06822.
(26) Griffith, E. C.; Carpenter, B. K.; Shoemaker, R. K.; Vaida, V. Photochemistry of Aqueous Pyruvic Acid. *Proc. Natl. Acad. Sci. U.S.A.* **2013**, *110*, 11714.
(27) Bernard, F.; Ciuraru, R.; Boréave, A.; George, C. Photosensitized Formation of Secondary Organic Aerosols above the Air/Water Interface. *Environ. Sci. Technol.* **2016**, *50*, 8678−8686.
(28) Rapf, R. J.; Perkins, R. J.; Dooley, M. R.; Kroll, J. A.; Carpenter, B. K.; Vaida, V. Environmental Processing of Lipids Driven by Aqueous Photochemistry of α-Keto Acids. *ACS Cent. Sci.* **2018**, *4*, 624−630.
(29) Galloway, M. M.; Powelson, M. H.; Sedehi, N.; Wood, S. E.; Millage, K. D.; Kononenko, J. A.; Rynaski, A. D.; De Haan, D. O. Secondary Organic Aerosol Formation during Evaporation of Droplets Containing Atmospheric Aldehydes, Amines, and Ammonium Sulfate. *Environ. Sci. Technol.* **2014**, *48*, 14417−14425.
(30) De Haan, D. O.; Corrigan, A. L.; Tolbert, M. A.; Jimenez, J. L.; Wood, S. E.; Turley, J. J. Secondary Organic Aerosol Formation by Self-Reactions of Methylglyoxal and Glyoxal in Evaporating Droplets. *Environ. Sci. Technol.* **2009**, *43*, 8184−8190.
(31) Surratt, J. D.; Chan, A. W. H.; Eddingsaas, N. C.; Chan, M.; Loza, C. L.; Kwan, A. J.; Hersey, S. P.; Flagan, R. C.; Wennberg, P. O.; Seinfeld, J. H. Reactive Intermediates Revealed in Secondary Organic Aerosol Formation from Isoprene. *Proc. Natl. Acad. Sci.* **2010**, *107*, 6640−6645.
(32) Lee, A. K. Y.; Zhao, R.; Li, R.; Liggio, J.; Li, S.-M.; Abbatt, J. P. D. Formation of Light Absorbing Organo-Nitrogen Species from Evaporation of Droplets Containing Glyoxal and Ammonium Sulfate. *Environ. Sci. Technol.* **2013**, *47*, 12819−12826.
(33) Ervens, B. Progress and Problems in Modeling Chemical Processing in Cloud Droplets and Wet Aerosol Particles. In *Multiphase Environmental Chemistry in the Atmosphere*; ACS Symposium Series; American Chemical Society, 2018; Vol. *1299*, pp 327−345.
(34) Donahue, N. M.; Kroll, J. H.; Pandis, S. N.; Robinson, A. L. A Two-Dimensional Volatility Basis Set − Part 2: Diagnostics of Organic-Aerosol Evolution. *Atmos. Chem. Phys.* **2012**, *12*, 615−634.
(35) Loeffler, K. W.; Koehler, C. A.; Paul, N. M.; De Haan, D. O. Oligomer Formation in Evaporating Aqueous Glyoxal and Methyl Glyoxal Solutions. *Environ. Sci. Technol.* **2006**, *40*, 6318−6323.
(36) Barsanti, K. C.; Kroll, J. H.; Thornton, J. A. Formation of Low-Volatility Organic Compounds in the Atmosphere: Recent Advancements and Insights. *J. Phys. Chem. Lett.* **2017**, *8*, 1503−1511.
(37) Girod, M.; Moyano, E.; Campbell, D. I.; Cooks, R. G. Accelerated Bimolecular Reactions in Microdroplets Studied by Desorption Electrospray Ionization Mass Spectrometry. *Chem. Sci.* **2011**, *2*, 501−510.
(38) Marsh, B. M.; Iyer, K.; Cooks, R. G. Reaction Acceleration in Electrospray Droplets: Size, Distance, and Surfactant Effects. *J. Am. Soc. Mass Spectrom.* **2019**, *30*, 2022.
(39) Bain, R. M.; Pulliam, C. J.; Thery, F.; Cooks, R. G. Accelerated Chemical Reactions and Organic Synthesis in Leidenfrost Droplets. *Angew. Chem., Int. Ed.* **2016**, *55*, 10478−10482.
(40) Badu-Tawiah, A. K.; Campbell, D. I.; Cooks, R. G. Reactions of Microsolvated Organic Compounds at Ambient Surfaces: Droplet Velocity, Charge State, and Solvent Effects. *J. Am. Soc. Mass Spectrom.* **2012**, *23*, 1077−1084.
(41) Nguyen, T. B.; Lee, P. B.; Updyke, K. M.; Bones, D. L.; Laskin, J.; Laskin, A.; Nizkorodov, S. A. Formation of Nitrogen- and Sulfur-Containing Light-Absorbing Compounds Accelerated by Evaporation of Water from Secondary Organic Aerosols. *J. Geophys. Res.: Atmos.* **2012**, *117*, D01207.
(42) Li, Y.; Yan, X.; Cooks, R. G. The Role of the Interface in Thin Film and Droplet Accelerated Reactions Studied by Competitive Substituent Effects. *Angew. Chem., Int. Ed.* **2016**, *55*, 3433−3437.
(43) Zhong, J.; Kumar, M.; Francisco, J. S.; Zeng, X. C. Insight into Chemistry on Cloud/Aerosol Water Surfaces. *Acc. Chem. Res.* **2018**, *51*, 1229−1237.
(44) Eugene, A. J.; Pillar, E. A.; Colussi, A. J.; Guzman, M. I. Enhanced Acidity of Acetic and Pyruvic Acids on the Surface of Water. *Langmuir* **2018**, *34*, 9307−9313.
(45) Narayan, S.; Muldoon, J.; Finn, M. G.; Fokin, V. V.; Kolb, H. C.; Sharpless, K. B. "On Water": Unique Reactivity of Organic Compounds in Aqueous Suspension. *Angew. Chem., Int. Ed.* **2005**, *44*, 3275−3279.

https://dx.doi.org/10.1021/acsearthspacechem.0c00044
ACS Earth Space Chem. 2020, 4, 741−749

(46) Donaldson, D. J.; Vaida, V. The Influence of Organic Films at the Air−Aqueous Boundary on Atmospheric Processes. *Chem. Rev.* **2006**, *106*, 1445−1461.
(47) Nishino, N.; Hollingsworth, S. A.; Stern, A. C.; Roeselová, M.; Tobias, D. J.; Finlayson-Pitts, B. J. Interactions of Gaseous HNO3 and Water with Individual and Mixed Alkyl Self-Assembled Monolayers at Room Temperature. *Phys. Chem. Chem. Phys.* **2014**, *16*, 2358−2367.
(48) Wingen, L. M.; Moskun, A. C.; Johnson, S. N.; Thomas, J. L.; Roeselová, M.; Tobias, D. J.; Kleinman, M. T.; Finlayson-Pitts, B. J. Enhanced Surface Photochemistry in Chloride−Nitrate Ion Mixtures. *Phys. Chem. Chem. Phys.* **2008**, *10*, 5668−5677.
(49) Stefan, M. I.; Bolton, J. R. Reinvestigation of the Acetone Degradation Mechanism in Dilute Aqueous Solution by the UV/H2O2 Process. *Environ. Sci. Technol.* **1999**, *33*, 870−873.
(50) Kawamura, K.; Tachibana, E.; Okuzawa, K.; Aggarwal, S. G.; Kanaya, Y.; Wang, Z. F. High Abundances of Water-Soluble Dicarboxylic Acids, Ketocarboxylic Acids and α-Dicarbonyls in the Mountaintop Aerosols over the North China Plain during Wheat Burning Season. *Atmos. Chem. Phys.* **2013**, *13*, 8285−8302.
(51) Talbot, R. W.; Andreae, M. O.; Berresheim, H.; Jacob, D. J.; Beecher, K. M. Sources and Sinks of Formic, Acetic, and Pyruvic Acids over Central Amazonia: 2. Wet Season. *J. Geophys. Res.: Atmos.* **1990**, *95*, 16799−16811.
(52) Praplan, A. P.; Hegyi-Gaeggeler, K.; Barmet, P.; Pfaffenberger, L.; Dommen, J.; Baltensperger, U. Online Measurements of Water-Soluble Organic Acids in the Gas and Aerosol Phase from the Photooxidation of 1,3,5-Trimethylbenzene. *Atmos. Chem. Phys.* **2014**, *14*, 8665−8677.
(53) Mattila, J. M.; Brophy, P.; Kirkland, J.; Hall, S.; Ullmann, K.; Fischer, E. V.; Brown, S.; McDuffie, E.; Tevlin, A.; Farmer, D. K. Tropospheric Sources and Sinks of Gas-Phase Acids in the Colorado Front Range. *Atmos. Chem. Phys.* **2018**, *18*, 12315−12327.
(54) Andino, J. M.; Smith, J. N.; Flagan, R. C.; Goddard, W. A.; Seinfeld, J. H. Mechanism of Atmospheric Photooxidation of Aromatics: A Theoretical Study. *J. Phys. Chem.* **1996**, *100*, 10967−10980.
(55) Veres, P.; Roberts, J. M.; Burling, I. R.; Warneke, C.; de Gouw, J.; Yokelson, R. J. Measurements of Gas-Phase Inorganic and Organic Acids from Biomass Fires by Negative-Ion Proton-Transfer Chemical-Ionization Mass Spectrometry. *J. Geophys. Res.: Atmos.* **2010**, *115*, D23302.
(56) Reed Harris, A. E.; Pajunoja, A.; Cazaunau, M.; Gratien, A.; Pangui, E.; Monod, A.; Griffith, E. C.; Virtanen, A.; Doussin, J.-F.; Vaida, V. Multiphase Photochemistry of Pyruvic Acid under Atmospheric Conditions. *J. Phys. Chem. A* **2017**, *121*, 3327−3339.
(57) Andreae, M. O.; Talbot, R. W.; Li, S.-M. Atmospheric Measurements of Pyruvic and Formic Acid. *J. Geophys. Res.: Atmos.* **1987**, *92*, 6635−6641.
(58) Guzmán, M. I.; Colussi, A. J.; Hoffmann, M. R. Photoinduced Oligomerization of Aqueous Pyruvic Acid. *J. Phys. Chem. A* **2006**, *110*, 3619−3626.
(59) Schaefer, T.; Schindelka, J.; Hoffmann, D.; Herrmann, H. Laboratory Kinetic and Mechanistic Studies on the OH-Initiated Oxidation of Acetone in Aqueous Solution. *J. Phys. Chem. A* **2012**, *116*, 6317−6326.
(60) Healy, R. M.; Wenger, J. C.; Metzger, A.; Duplissy, J.; Kalberer, M.; Dommen, J. Gas/Particle Partitioning of Carbonyls in the Photooxidation of Isoprene and 1,3,5-Trimethylbenzene. *Atmos. Chem. Phys.* **2008**, *8*, 3215−3230.
(61) Berglund, R. N.; Liu, B. Y. H. Generation of Monodisperse Aerosol Standards. *Environ. Sci. Technol.* **1973**, *7*, 147−153.
(62) Werner, F.; Ditas, F.; Siebert, H.; Simmel, M.; Wehner, B.; Pilewskie, P.; Schmeissner, T.; Shaw, R. A.; Hartmann, S.; Wex, H.; Roberts, G. C.; Wendisch, M. Twomey Effect Observed from Collocated Microphysical and Remote Sensing Measurements over Shallow Cumulus. *J. Geophys. Res.: Atmos.* **2014**, *119*, 1534−1545.
(63) Barr, E. B.; Carpenter, R. L.; Newton, G. J. Improved Liquid Feed System for the Berglund-Liu Vibrating Orifice Monodisperse Aerosol Generator. *Environ. Sci. Technol.* **1984**, *18*, 721−723.
(64) Devarakonda, V.; Ray, A. K.; Kaiser, T.; Schweiger, G. Vibrating Orifice Droplet Generator for Studying Fast Processes Associated with Microdroplets. *Aerosol Sci. Technol.* **1998**, *28*, 531−547.
(65) Mavrogiannis, N.; Ibo, M.; Fu, X.; Crivellari, F.; Gagnon, Z. Microfluidics Made Easy: A Robust Low-Cost Constant Pressure Flow Controller for Engineers and Cell Biologists. *Biomicrofluidics* **2016**, *10*, 034107.
(66) Petters, M. D.; Kreidenweis, S. M.; Prenni, A. J.; Sullivan, R. C.; Carrico, C. M.; Koehler, K. A.; Ziemann, P. J. Role of Molecular Size in Cloud Droplet Activation. *Geophys. Res. Lett.* **2009**, *36*, L22801.
(67) Petters, S. S.; Pagonis, D.; Claflin, M. S.; Levin, E. J. T.; Petters, M. D.; Ziemann, P. J.; Kreidenweis, S. M. Hygroscopicity of Organic Compounds as a Function of Carbon Chain Length and Carboxyl, Hydroperoxy, and Carbonyl Functional Groups. *J. Phys. Chem. A* **2017**, *121*, 5164−5174.
(68) Davies, J. F.; Haddrell, A. E.; Reid, J. P. Time-Resolved Measurements of the Evaporation of Volatile Components from Single Aerosol Droplets. *Aerosol Sci. Technol.* **2012**, *46*, 666−677.
(69) Rovelli, G.; Miles, R. E. H.; Reid, J. P.; Clegg, S. L. Accurate Measurements of Aerosol Hygroscopic Growth over a Wide Range in Relative Humidity. *J. Phys. Chem. A* **2016**, *120*, 4376−4388.
(70) Su, Y.-Y.; Marsh, A.; Haddrell, A. E.; Li, Z.-M.; Reid, J. P. Evaporation Kinetics of Polyol Droplets: Determination of Evaporation Coefficients and Diffusion Constants. *J. Geophys. Res.: Atmos.* **2017**, *122*, 12317−12334.
(71) Dawson, K. W.; Petters, M. D.; Meskhidze, N.; Petters, S. S.; Kreidenweis, S. M. Hygroscopic Growth and Cloud Droplet Activation of Xanthan Gum as a Proxy for Marine Hydrogels. *J. Geophys. Res.: Atmos.* **2016**, *121*, 11803−11818.
(72) Tomaz, S.; Cui, T.; Chen, Y.; Sexton, K. G.; Roberts, J. M.; Warneke, C.; Yokelson, R. J.; Surratt, J. D.; Turpin, B. J. Photochemical Cloud Processing of Primary Wildfire Emissions as a Potential Source of Secondary Organic Aerosol. *Environ. Sci. Technol.* **2018**, *52*, 11027−11037.
(73) van Pinxteren, D.; Fomba, K. W.; Mertes, S.; Müller, K.; Spindler, G.; Schneider, J.; Lee, T.; Collett, J. L.; Herrmann, H. Cloud Water Composition during HCCT-2010: Scavenging Efficiencies, Solute Concentrations, and Droplet Size Dependence of Inorganic Ions and Dissolved Organic Carbon. *Atmos. Chem. Phys.* **2016**, *16*, 3185−3205.
(74) Deguillaume, L.; Charbouillot, T.; Joly, M.; Vaïtilingom, M.; Parazols, M.; Marinoni, A.; Amato, P.; Delort, A.-M.; Vinatier, V.; Flossmann, A.; Chaumerliac, N.; Pichon, J. M.; Houdier, S.; Laj, P.; Sellegri, K.; Colomb, A.; Brigante, M.; Mailhot, G. Classification of Clouds Sampled at the Puy de Dôme (France) Based on 10 Yr of Monitoring of Their Physicochemical Properties. *Atmos. Chem. Phys.* **2014**, *14*, 1485−1506.
(75) Lim, Y. B.; Tan, Y.; Turpin, B. J. Chemical Insights, Explicit Chemistry, and Yields of Secondary Organic Aerosol from OH Radical Oxidation of Methylglyoxal and Glyoxal in the Aqueous Phase. *Atmos. Chem. Phys.* **2013**, *13*, 8651−8667.
(76) Herrmann, H.; Hoffmann, D.; Schaefer, T.; Bräuer, P.; Tilgner, A. Tropospheric Aqueous-Phase Free-Radical Chemistry: Radical Sources, Spectra, Reaction Kinetics and Prediction Tools. *ChemPhysChem* **2010**, *11*, 3796−3822.
(77) Arakaki, T.; Anastasio, C.; Kuroki, Y.; Nakajima, H.; Okada, K.; Kotani, Y.; Handa, D.; Azechi, S.; Kimura, T.; Tsuhako, A.; Miyagi, Y. A General Scavenging Rate Constant for Reaction of Hydroxyl Radical with Organic Carbon in Atmospheric Waters. *Environ. Sci. Technol.* **2013**, *47*, 8196−8203.
(78) Ahn, K.-H.; Liu, B. Y. H. Particle Activation and Droplet Growth Processes in Condensation Nucleus Counter—I. Theoretical Background. *J. Aerosol Sci.* **1990**, *21*, 249−261.
(79) Bilde, M.; Svenningsson, B.; Mønster, J.; Rosenørn, T. Even−Odd Alternation of Evaporation Rates and Vapor Pressures of C3−C9 Dicarboxylic Acid Aerosols. *Environ. Sci. Technol.* **2003**, *37*, 1371−1378.

https://dx.doi.org/10.1021/acsearthspacechem.0c00044
ACS Earth Space Chem. 2020, 4, 741−749

(80) Hinds, W. C. *Aerosol Technology: Properties, Behavior, and Measurement of Airborne Particles*, 2nd ed.; John Wiley and Sons: New York, 1999.
(81) Davis, E. J.; Ray, A. K. Submicron Droplet Evaporation in the Continuum and Non-Continuum Regimes. *J. Aerosol Sci.* **1978**, *9*, 411−422.
(82) Hirschfelder, J. O.; Curtiss, C. F.; Bird, R. B. *Molecular Theory of Gases and Liquids*; Wiley, 1967.
(83) Lim, H.-J.; Carlton, A. G.; Turpin, B. J. Isoprene Forms Secondary Organic Aerosol Through Cloud Processing: Model Simulations. *Environ. Sci. Technol.* **2005**, *39*, 4441−4446.
(84) Suda, S. R.; Petters, M. D. Accurate Determination of Aerosol Activity Coefficients at Relative Humidities up to 99% Using the Hygroscopicity Tandem Differential Mobility Analyzer Technique. *Aerosol Sci. Technol.* **2013**, *47*, 991−1000.
(85) Suda, S. R.; Petters, M. D.; Matsunaga, A.; Sullivan, R. C.; Ziemann, P. J.; Kreidenweis, S. M. Hygroscopicity Frequency Distributions of Secondary Organic Aerosols. *J. Geophys. Res.: Atmos.* **2012**, *117*, D04207.
(86) Pocker, Y.; Meany, J. E.; Nist, B. J.; Zadorojny, C. Reversible Hydration of Pyruvic Acid. I. Equilibrium Studies. *J. Phys. Chem.* **1969**, *73*, 2879−2882.
(87) Ziemann, P. J.; Atkinson, R. Kinetics, Products, and Mechanisms of Secondary Organic Aerosol Formation. *Chem. Soc. Rev.* **2012**, *41*, 6582−6605.
(88) Herrmann, H.; Schaefer, T.; Tilgner, A.; Styler, S. A.; Weller, C.; Teich, M.; Otto, T. Tropospheric Aqueous-Phase Chemistry: Kinetics, Mechanisms, and Its Coupling to a Changing Gas Phase. *Chem. Rev.* **2015**, *115*, 4259−4334.
(89) Chan, A. W. H.; Chan, M. N.; Surratt, J. D.; Chhabra, P. S.; Loza, C. L.; Crounse, J. D.; Yee, L. D.; Flagan, R. C.; Wennberg, P. O.; Seinfeld, J. H. Role of Aldehyde Chemistry and NOx Concentrations in Secondary Organic Aerosol Formation. *Atmos. Chem. Phys.* **2010**, *10*, 7169−7188.
(90) Jaoui, M.; Edney, E. O.; Kleindienst, T. E.; Lewandowski, M.; Offenberg, J. H.; Surratt, J. D.; Seinfeld, J. H. Formation of Secondary Organic Aerosol from Irradiated α-Pinene/Toluene/NOx Mixtures and the Effect of Isoprene and Sulfur Dioxide. *J. Geophys. Res.: Atmos.* **2008**, *113*, D09303.
(91) Liggio, J.; Li, S.-M.; McLaren, R. Heterogeneous Reactions of Glyoxal on Particulate Matter: Identification of Acetals and Sulfate Esters. *Environ. Sci. Technol.* **2005**, *39*, 1532−1541.
(92) Sanz, M. T.; Gmehling, J. Esterification of Acetic Acid with Isopropanol Coupled with Pervaporation: Part I: Kinetics and Pervaporation Studies. *Chem. Eng. J.* **2006**, *123*, 1−8.
(93) Rathod, A. P.; Wasewar, K. L.; Sonawane, S. S. Enhancement of Esterification Reaction by Pervaporation Reactor: An Intensifying Approach. *Procedia Eng.* **2013**, *51*, 330−334.
(94) Barsanti, K. C.; Pankow, J. F. Thermodynamics of the Formation of Atmospheric Organic Particulate Matter by Accretion Reactions—Part 1: Aldehydes and Ketones. *Atmos. Environ.* **2004**, *38*, 4371−4382.
(95) Tong, C.; Blanco, M.; Goddard, W. A.; Seinfeld, J. H. Secondary Organic Aerosol Formation by Heterogeneous Reactions of Aldehydes and Ketones: A Quantum Mechanical Study. *Environ. Sci. Technol.* **2006**, *40*, 2333−2338.
(96) Krizner, H. E.; De Haan, D. O.; Kua, J. Thermodynamics and Kinetics of Methylglyoxal Dimer Formation: A Computational Study. *J. Phys. Chem. A* **2009**, *113*, 6994−7001.
(97) Rapf, R. J.; Dooley, M. R.; Kappes, K.; Perkins, R. J.; Vaida, V. PH Dependence of the Aqueous Photochemistry of α-Keto Acids. *J. Phys. Chem. A* **2017**, *121*, 8368−8379.
(98) Perkins, R. J.; Shoemaker, R. K.; Carpenter, B. K.; Vaida, V. Chemical Equilibria and Kinetics in Aqueous Solutions of Zymonic Acid. *J. Phys. Chem. A* **2016**, *120*, 10096−10107.
(99) Otto, T.; Stieger, B.; Mettke, P.; Herrmann, H. Tropospheric Aqueous-Phase Oxidation of Isoprene-Derived Dihydroxycarbonyl Compounds. *J. Phys. Chem. A* **2017**, *121*, 6460−6470.
(100) Mellouki, A.; Mu, Y. On the Atmospheric Degradation of Pyruvic Acid in the Gas Phase. *Atmospheric Photochem.* **2003**, *157*, 295−300.
(101) Sander, R. Compilation of Henry's Law Constants (Version 4.0) for Water as Solvent. *Atmos. Chem. Phys.* **2015**, *15*, 4399−4981.
(102) Epstein, S. A.; Nizkorodov, S. A. A Comparison of the Chemical Sinks of Atmospheric Organics in the Gas and Aqueous Phase. *Atmos. Chem. Phys.* **2012**, *12*, 8205−8222.
(103) Stull, D. R. Inorganic Compounds. *Ind. Eng. Chem.* **1947**, *39*, 540−550.
(104) Emel'yanenko, V. N.; Turovtsev, V. V.; Fedina, Y. A. Thermodynamic Properties of Pyruvic Acid and Its Methyl Ester. *Thermochim. Acta* **2018**, *665*, 70−75.
(105) Soonsin, V.; Zardini, A. A.; Marcolli, C.; Zuend, A.; Krieger, U. K. The Vapor Pressures and Activities of Dicarboxylic Acids Reconsidered: The Impact of the Physical State of the Aerosol. *Atmos. Chem. Phys.* **2010**, *10*, 11753−11767.
(106) Booth, A. M.; Barley, M. H.; Topping, D. O.; McFiggans, G.; Garforth, A.; Percival, C. J. Solid State and Sub-Cooled Liquid Vapour Pressures of Substituted Dicarboxylic Acids Using Knudsen Effusion Mass Spectrometry (KEMS) and Differential Scanning Calorimetry. *Atmos. Chem. Phys.* **2010**, *10*, 4879−4892.
(107) Paciga, A. L.; Riipinen, I.; Pandis, S. N. Effect of Ammonia on the Volatility of Organic Diacids. *Environ. Sci. Technol.* **2014**, *48*, 13769−13775.
(108) Pankow, J. F.; Asher, W. E. SIMPOL.1: A Simple Group Contribution Method for Predicting Vapor Pressures and Enthalpies of Vaporization of Multifunctional Organic Compounds. *Atmos. Chem. Phys.* **2008**, *8*, 2773−2796.
(109) Gordon, B. P.; Moore, F. G.; Scatena, L. F.; Richmond, G. L. On the Rise: Experimental and Computational VSFS Studies of Pyruvic Acid and Its Surface Active Oligomer Species at the Air-Water Interface. *J. Phys. Chem. A* **2019**, *123*, 10609.
(110) Bilde, M.; Barsanti, K.; Booth, M.; Cappa, C. D.; Donahue, N. M.; Emanuelsson, E. U.; McFiggans, G.; Krieger, U. K.; Marcolli, C.; Topping, D.; Ziemann, P.; Barley, M.; Clegg, S.; Dennis-Smither, B.; Hallquist, M.; Hallquist, Å. M.; Khlystov, A.; Kulmala, M.; Mogensen, D.; Percival, C. J.; Pope, F.; Reid, J. P.; Ribeiro da Silva, M. A. V.; Rosenoern, T.; Salo, K.; Soonsin, V. P.; Yli-Juuti, T.; Prisle, N. L.; Pagels, J.; Rarey, J.; Zardini, A. A.; Riipinen, I. Saturation Vapor Pressures and Transition Enthalpies of Low-Volatility Organic Molecules of Atmospheric Relevance: From Dicarboxylic Acids to Complex Mixtures. *Chem. Rev.* **2015**, *115*, 4115−4156.

https://dx.doi.org/10.1021/acsearthspacechem.0c00044
ACS Earth Space Chem. 2020, 4, 741−749